

FADE: Selective Forgetting via Sparse LoRA and Self-Distillation

Carolina R. Kelsch* Leonardo S. B. Pereira* Natnael Mola*
 Luis H. Arribas Juan C. S. M. Avedillo

February 10, 2026

Abstract

Machine Unlearning aims to remove the influence of specific data or concepts from trained models while preserving overall performance, a capability increasingly required by data protection regulations and responsible AI practices. Despite recent progress, unlearning in text-to-image diffusion models remains challenging due to high computational costs and the difficulty of balancing effective forgetting with retention of unrelated concepts. We introduce FADE (Fast Adapter for Data Erasure), a two-stage unlearning method for image generation that combines parameter localization with self-distillation. FADE first identifies parameters most responsible for the forget set using gradient-based saliency and constrains updates through sparse LoRA adapters, ensuring lightweight, localized modifications. In a second stage, FADE applies a self-distillation objective that overwrites the forgotten concept with a user-defined surrogate while preserving behavior on retained data. The resulting adapters are memory-efficient, reversible, and can be merged or removed at runtime, enabling flexible deployment in production systems. We evaluated FADE on the UnlearnCanvas benchmark and conducted ablation studies on Imagenette, Labeled Faces in the Wild, AtharvaTaras Dog Breeds Dataset, and SUN Attributes datasets, demonstrating State-of-the-Art unlearning performance with fine-grained control over the forgetting–retention trade-off. Our results demonstrate that FADE achieves strong concept erasure and high retainability across various domains, making it a suitable solution for selective unlearning in diffusion-based image generation models.

1 Introduction

Machine Unlearning (MU) is the area of Machine Learning (ML) that studies the removal of data from an Artificial Intelligence (AI) system, making the system unlearn a concept or forget what it learned from a specific data point [1]. This area has been given more importance over the past few years with the advancement of some regulations that provide users with the right to have more control over the data they generate, such as the General Data Protection Regulation (GDPR) in the EU [2]. With that in force, companies need to be able to remove from their trained models data from specific users. Besides that, MU can be used for mitigating biases [3] and improving model interpretability [4], thus contributing to greater efforts towards safe and responsible AI.

The field has evolved in a modality-siloed manner, where most methods are evaluated either on textual tasks, or on visual classification, or on text-to-image generation, but rarely across modalities [5]. In such a fragmented scenario, image generation tasks have lagged behind in the pace of development, partly because diffusion models require substantially higher compute to fine-tune [6], and partly because evaluating unlearning in generation is intrinsically harder [7].

Existing unlearning methods for image generation struggle to balance the removal of the target concept with the preservation of unrelated capabilities [1, 8]. This balance is essential: aggressive updates often trigger collateral forgetting, where semantically or statistically adjacent concepts degrade together, reducing the practical utility of the model. Furthermore, most current approaches provide limited mechanisms to control the trade-off between forgetting and retention [9], which restricts their applicability in real-world settings that require selective and explainable unlearning at scale.

*These authors contributed equally to this work.

In this work, we present a new MU method for image generation named Fast Adapter for Data Erasure (FADE), a two-stage unlearning method that first identifies the subset of parameters most responsible for the forget set through a per-weight saliency mask and then applies a lightweight overwrite procedure using self-distillation. The update is implemented through sparse LoRA adapters, which restrict all modifications to the selected weights and keep the memory footprint low; Moreover, the adapter can be merged or removed at runtime, enabling reversible deployment. FADE allows the user to move along the Pareto front of solutions, deciding how aggressively forgetting should be performed and at what expense of retention.

We evaluate FADE on the UnlearnCanvas benchmark [10], alongside small-scale ablation studies on the dataset Imagenette [11], Labeled Faces in the Wild (LFW) [12], AtharvaTaras Dog Breeds Dataset [13], and Scene UNderstanding (SUN) Attributes [14]. FADE improves significantly over the State-of-the-Art while allowing an unprecedented amount of control over how forgetting and retaining are balanced. Furthermore, our method results in lightweight modules that can be added and removed from a model at runtime, respectively forgetting or restoring the original behavior, easing its usage in production environments.

2 Literature Review

2.1 Diffusion Models

Diffusion models have become the dominant architecture for text-to-image generation, achieving high sample quality and strong semantic alignment with natural-language prompts [6, 15]. They generate images by iteratively denoising a latent variable, conditioned on text embeddings produced by a large language encoder, typically via cross-attention layers. Because semantic information is distributed across many denoising steps and model blocks, modifying the behavior of a diffusion model requires careful control: even small parameter updates can propagate through the iterative sampling process and alter unrelated visual concepts.

Stable Diffusion [15] follows the latent-diffusion design, where denoising operates in a compressed latent space rather than pixel space, enabling training and fine-tuning at manageable computational cost. Its architecture consists of a UNet backbone for iterative denoising, a frozen CLIP text encoder for conditioning, and a variational autoencoder (VAE) for mapping between images and latent representations.

2.2 Parameter-Efficient Fine-Tuning (PEFT)

Parameter-Efficient Fine-Tuning (PEFT) refers to techniques that adapt large pre-trained models to downstream tasks while updating only a small fraction of parameters, thus significantly reducing computation, memory, and storage costs relative to full fine-tuning [16]. A prominent instantiation is LoRA (Low-Rank Adaptation), which freezes the original model weights and injects trainable low-rank matrices into selected layers, allowing the adaptation to be expressed as the product of two small matrices rather than modifying the full weight matrix [17].

Beyond standard LoRA, the work of [18] introduces SparseLoRA, a variation designed to constrain adaptation so that only a small, deliberately selected subset of weights in the frozen model is modified. Instead of applying a dense low-rank update across an entire layer, the adapter update is structurally restricted by a fixed binary pattern, ensuring that parameter changes remain highly localized and affect only a minimal portion of the weight tensor. This transforms the adapter into a sparse, location-controlled refinement mechanism — still low-rank, but now also spatially selective — allowing downstream tuning to operate through precise, fine-grained modifications.

2.3 Machine Unlearning

The unlearning task can be formalized as the modification of a ML model in order to remove the influence and the knowledge learned from part of the dataset, denoted as *forget set* (D_f), while retaining knowledge obtained from training in the remaining data, denoted as *retain set* (D_r) [19]. Optionally, may be specified a set specifying the concept to which prompts referring to D_f should map, henceforth referred to as *overwrite set* (D_o) [20].

Even though unlearning methods vary slightly in how these concepts are defined, this notation will be used uniformly throughout this paper. The most common variations for representing these concepts are in terms of a dataset (a set of images), a set of prompts used to generate images with a generative model (also known as Data-Free Unlearning [21]), or metadata (for example, a textual description of D_f or some of its properties [22]).

Some methods, such as Score Forgetting Distillation (SFD) [23], indirectly represent metadata about D_f through the engineer’s choice of D_o . For example, if we want to forget Brad Pitt and choose “middle-aged man” as the concept to overwrite, we implicitly indicate to the model that Brad Pitt is a middle-aged man. However, these methods do not allow D_o to arbitrarily describe D_f , since doing so would prevent any forgetting. Similarly, D_o can be used to compensate for the absence of D_r in cases where D_r is unknown or too difficult to specify [21]; in such cases, D_o often lies within D_r and close to or intersecting with D_f .

SalUn [7], on the other hand, does not use a replacement concept at all, utilizing only on D_f and D_r . It applies a threshold γ to D_f to create a mask of salient weights, which encodes knowledge of the forget set, and then fine-tunes only these weights. Furthermore, D_f and D_r can be specified either as a dataset of real images or as a set of prompts used to generate images.

2.3.1 Information-theoretic approaches

Other early developments in the MU field used the Fisher Information Matrix (FIM) to obtain how much information a parameter contains about a specific sample [24], thus allowing targeted forgetting of D_f without harming other tasks. For a network of d parameters, this matrix has size $d \times d$, in which each element ij is calculated by $F_{ij}(\theta) = \mathbb{E} \left[\frac{\partial \log p(x|\theta)}{\partial \theta_i} \frac{\partial \log p(x|\theta)}{\partial \theta_j} \right]$, where $p(x|\theta)$ is the probability of obtaining x sampling from a distribution with θ as parameter. In the context of second-order optimization, the FIM can be used to approximate the Hessian, which further expands the applicability of these methods even beyond the field of MU.

However, since the FIM scales quadratically with the model size, it may have billions of elements for most modern ML models, thus becoming infeasible to store and compute it exactly. Several approximations can be used to decrease the computational requirements [24, 25, 26, 27], such as calculating just the diagonal of the FIM [24].

The method proposed by [28], often referred to as Fisher Forgetting or Scrubbing, perturbs the parameters by applying to them an additive Gaussian noise, whose covariance is obtained with the FIM calculated over the forget set. The method does not require access to the original dataset, as long as is computed and saved, making it particularly suitable for scenarios where data is no longer available but forgetting is mandated. The Kronecker-factorized approximation [25] was used to approximate the FIM, and the hyperparameter lambda was introduced to control the amount of noise (that empirically trades off forgetting with the increase in error).

The method of Influence Unlearning (IU) [29], also known as Projective Residual Update, obtains the unlearned model by adding the original model with an update calculated over the forget dataset by using the inverse of the Hessian. For practical purposes, the Hessian was approximated by the FIM by leveraging the Levenberg-Marquardt approximation, and the FIM is then analytically calculated.

2.3.2 Sparse-update approaches

Weight sparsity, first formalized in the Lottery Ticket Hypothesis [30], has been repeatedly adopted in MU as a mechanism to constrain parameter updates and limit collateral forgetting. In this setting, sparsity is treated as a saliency or “location” map [31]: the unlearning algorithm updates only a selected subset of parameters, ideally those most responsible for representing the forget set, while freezing the rest of the network. The rationale is simple: restricting the update space preserves unrelated concepts and helps maintain global model behavior. Despite legitimate criticism about the stability and interpretability of saliency-based selection [31], several works report measurable reductions in unintended forgetting when such mechanisms are used [7, 8].

Sparsity can be enforced at different granularities. Coarse approaches operate at the module or block level, selecting which layers are allowed to update (e.g., only attention blocks, only cross-attention, etc.), with [8] showing that module-level gating can already suppress collateral forgetting. Fine-grained approaches instead compute per-weight importance scores and update only the highest-saliency weights [7, 32, 22, 33], allowing a more targeted unlearning but at the cost of higher book-

keeping and sensitivity to noise in gradient-based saliency. A related strategy prunes the model before applying the unlearning step [34], on the hypothesis that a sparser base model exposes a more interpretable and stable subnetwork for subsequent forgetting. Overall, coarse sparsity tends to be simpler and more robust but provides weaker control, whereas fine-grained sparsity offers greater specificity at the risk of overfitting the saliency signal.

2.3.3 Distillation-based approaches

Ideas originating from knowledge distillation [35] have been adapted to MU as a mechanism for constraining the updated model to remain close to the behavior of a reference (typically frozen) model while selectively altering its predictions on the forget set. Instead of modifying parameters through explicit gradient ascent or information-theoretic corrections, these methods transfer the behavior of a suitably defined teacher model to a student model whose outputs are steered so that forgetting occurs while global model structure and generation quality are preserved [23].

Concept Ablation (CA) [20] applies a distillation-like update by explicitly projecting out concept-specific directions from the cross-attention activations of a diffusion model: the teacher is the original model, while the student is trained so that its cross-attention maps match the teacher after removing the subspace associated with the concept to be erased. Unlearn-Noise-Distill-on-Outputs (UNDO) [36] decouples forgetting and preservation by first applying an unlearning step and then distilling the resulting model back toward the behavior of the original model on the retain set. Partitioned Unlearning with Retraining Guarantee for Ensembles (PURGE) [37] extends this line by using constituent mapping and an incremental multi-teacher protocol, in which different semantic components of the teacher are distilled separately to avoid collapsing unrelated concepts. DEcoupLED Distillation To Erase (DELETE) [38], designed for image classification, performs logits-level separation: a mask splits the logits into forgetting and retention components, and distinct distillation targets are constructed to suppress the forgotten class while stabilizing all remaining classes.

Score Forgetting Distillation (SFD) [23] applies these principles to diffusion models in a slightly different manner: on retain prompts, the student is trained so that its predicted noise matches that of the frozen teacher; On forget prompts, however, the target is the frozen teacher conditioned on a replacement prompt. This introduces an explicit overwrite mechanism (sometimes referred to as alignment [21], mapping [39], among others), in which the method defines not only what should be forgotten, but what the model should generate instead (for example, replacing “Brad Pitt” with “middle-aged man”).

Although the overwrite mechanism was first formalized in this distillation setting, it is not tied to distillation and can be integrated with other unlearning families. Additionally, overwrite introduces an additional evaluation challenge: several metrics depend on the semantic relation between the forget concept and the generated images [40, 41], with distant replacements typically producing larger shifts in metric values. Furthermore, the choice of overwriting concept affects the robustness of the model, with semantically distant concepts reducing the likelihood of the unlearned concept re-emerging during fine-tuning. As a result, quantitative comparisons must document the overwrite choice explicitly, since it directly influences the numerical behavior of standard evaluation metrics [39] (as discussed in Section 2.3.5).

2.3.4 Usage of PEFT

Several recent works rely on PEFT for concept erasure in diffusion models [42, 43, 44, 45]. These methods treat the Parameter Efficient Module (PEM) as a low-rank carrier of the forgetting signal: because the low intrinsic dimensionality restricts the optimization path, the update tends to be more localized and less disruptive to global behavior. Most approaches attach modules to the attention or cross-attention projections, and use ranks varying between 4 and 32; However, to the best of our knowledge, no systematic review of best practices for Parameter Efficient Fine-Tuning (PEFT) in the context of unlearning exists to date.

Extending this basic idea, Mass Concept Erasure (MACE) [45] leverages the low memory footprint of each individual module in order to unlearn several concepts simultaneously. Their method trains one PEM per concept and, instead of sequentially merging them, performs a dedicated LoRA fusion stage. Using an additional closed-form objective, it integrates multiple modules into the base model so that the effect of each module is preserved while their mutual interference is minimized. This

enables simultaneous erasure of up to 100 concepts while maintaining strong specificity, establishing PEFT-based LoRA composition as a practical strategy for scalable multi-concept unlearning.

Another way of using PEFT mechanisms in unlearning is by training a PEM that intentionally contains the harmful concept, such that the generation can be suppressed or improved simply by subtracting this module or adding[3] (that is, multiplying the module weights by -1 or keeping them untouched, respectively). This PEM-composition view provides an explicit linearization of concept removal, enabling controlled erasure without large modifications to the full model.

2.3.5 Evaluation

Evaluation of unlearning in image generation models relies on quantitative measures that assess both the disappearance of the target concept and the preservation of the model’s generative ability on all other concepts. The two most commonly used metrics are the Fréchet Inception Distance (FID) [40] for measuring distributional quality and the CLIP-based similarity score (henceforth, CLIP-score) [41] for measuring semantic alignment. FID estimates how far the distribution of generated images deviates from a reference dataset, and it is typically computed on retain prompts to ensure that the unlearning procedure has not degraded global model quality. CLIP-score is computed separately on forget prompts and retain prompts. A decrease in similarity on the forget set indicates attenuation of the erased concept, whereas stability on the retain set indicates preservation of unrelated concepts. Some works additionally employ external classifiers or detectors [7] when the forgotten concept corresponds to a specific object, attribute, or safety-critical category, allowing a more precise quantification of whether the unwanted content persists. Efficiency indicators such as wall-clock unlearning time and memory usage are also reported in recent literature, reflecting the practical relevance of computational constraints.

To address the challenges of evaluating MU in image generation, UnlearnCanvas [10] provides a high-resolution stylized image dataset designed to assess the erasure of artistic styles and objects. A key feature of this benchmark is the application of dual supervision, where images are annotated with both style and object labels to allow for precise isolation of unlearning targets. This structure enables the rigorous evaluation of “in-domain” retainability (preserving generative capability for concepts within the same category (e.g., generating different objects in a retained style) versus “cross-domain” retainability, which measures the preservation of concepts across different categories (e.g., maintaining object fidelity when a specific style is removed). [10] further utilizes this framework to benchmark sequential unlearning, revealing significant degradation in retainability as unlearning requests accumulate.

While UnlearnCanvas focuses on the disentanglement of styles and objects, recent literature has expanded to multi-dimensional benchmarks that systematize evaluation across broader criteria. The IGMU framework [46] addresses the ambiguity of unlearning targets through CatIGMU, a hierarchical categorization system based on spatial-scope relationships (global vs. local) and perceptual attributes (abstract vs. concrete). To counter the unreliability of existing task-specific detectors, EvalIGMU [46] integrates a multi-source dataset to quantify forgetting and preservation with higher precision. Similarly, the Holistic Unlearning Benchmark (HUB) [47] evaluates methods across six dimensions: faithfulness, alignment, pinpoint-ness, multilingual robustness, attack robustness, and efficiency. By utilizing a large-scale dataset of 16,000 prompts per concept, the stdy of [47] provides empirical evidence that current methods fail to optimize all criteria simultaneously, necessitating trade-offs between erasure effectiveness and generative quality.

Targeting the specific domain of content safety, the method proposed in [48] provides an evaluation framework designed for Not-Safe-For-Work (NSFW) concept erasure. Rather than relying on generic safety filters, [48] utilizes fine-grained thematic annotations to analyze the decoupling of prompt toxicity from visual safety. This work evaluates the robustness of erasure methods against adversarial toxic prompts and investigates their sensitivity to training data scales, differentiating the performance characteristics of post-hoc correction methods versus parameter fine-tuning approaches.

One concerning aspect of MU is the possibility of unlearned concepts reappearing when the resulting model is subsequently fine-tuned, even with general or unrelated data [49, 39]. One hypothesis for the origin of this phenomenon is the projection overlap between the forgotten subspace and the fine-tuning gradient directions, combined with a curvature-limited sensitivity bound that amplifies updates in low-curvature subspaces [49]. This analysis posits that some degree of resurgence is inevitable given any nonzero overlap between the relevant subspaces [49].

To facilitate the qualitative analysis of unlearning results, the work of [50] develops a web-based

interactive application for exploring evaluation results of unlearned models. By providing several visualization options, such interactive interfaces democratize unlearning and invite a broader set of professionals to discuss the evaluation of MU.

3 Materials and methods

The experiments and development described in this work were executed on a NVIDIA Tesla V100-PCIE-16GB GPU and a NVIDIA Tensor Core A100-PCIE-40GB made available through the Pázmány Péter Catholic University High-Performance Computing cluster (Esztergom). Cluster access was performed between June and December 2025 via the institution Slurm scheduler (version 23.11.4) running on the operating system CentOS 8.10 “Green Obsidian”. We provisioned approximately 400 GPU hours for the reported experiments; using the Hungarian grid carbon intensity this corresponds to an estimated footprint of 60.23 kgCO₂e.

Code was written for Python 3.10 and relies on PyTorch 2.8, diffusers 0.30, transformers 4.55, peft 0.17, among other minor dependencies; model artifacts and checkpoints were managed using the Hugging Face Hub. The FADE implementation and the evaluation procedures used to calculate the reported metrics were published in the Vision-Unlearning library (version 0.1.6). Development and experiment orchestration used Poetry for dependency management, Apptainer for containerized execution, and a Makefile to automate common workflows.

For the comparative benchmark and the final evaluations we used the UnlearnCanvas benchmark as described in the Section 5. Controlled small-scale ablations were performed using the following tasks: forgetting an object from Imagenette dataset [11], containing 13394 images across 10 classes of objects; Unlearning one person from the dataset Labeled Faces in the Wild (LFW) [12], that is intended for studying unconstrained face recognition problems (in which there is little control over parameters such as position, pose, lighting, background, camera quality); Unlearning a dog breed from the dataset AtharvaTaras Dog Breeds Dataset [13], with 356 breeds recognized by the FCI (Fédération Cynologique Internationale) and containing 35 images for each breed; Unlearning a scene from the SUN Attributes [14] dataset, intended for fine-grained scene categorization and containing more than 14,000 images from 717 classes.

The utilized base models were Stable Diffusion v1.4 and v1.5. All evaluation metrics reported (CLIP alignment, FID, unlearning/retention accuracies, and runtime measurements) were produced either with the benchmark or with the built-in procedures of the Vision-Unlearning library to ensure that metric computation and dataset splits are reproducible and auditable.

4 Proposed method

Our method balances retaining and forgetting by following a 2-step procedure.

4.1 Knowledge location step

We ensure retention by restricting the update only to parameters that are relevant to the current forgetting task. This is achieved by calculating the subset W_f of weights whose saliency with respect to D_f is higher than a predefined threshold hyperparameter γ . Since this subset is likely much smaller than the entire parameter space W , a low-rank adapter is a suitable choice for performing the update.

In order for the adapter to only modify parameters related to W_f , we developed an approach inspired by SparsePEFT [18] in which the update space of the product BA is restricted by taking its Hadamard product with a boolean mask of W_f , during the entire training process. That is, $(BA) \odot (Saliency(W, D_f) > \gamma)$. This variation of SparsePEFT was released in a separate repository [51]. This approach performs a fine-grained per-weight masking. A possible variation of this method is to perform coarse-grained per-block masking. Both approaches are compared in the Section 6.1, and a literature review on the topic is provided in Section 2.3.2.

4.2 Distillation training step

The second step aims to erase from W_f the knowledge about D_f using self-distillation training, inspired by Score Forgetting Distillation [23] and Concept Ablation [20]. That is done by applying

forward diffusion to random time steps, for images and prompts from the retain set, and pass the noisy image and prompt to both the frozen U-net and the U-net to be fine-tuned, then the score predictions from both models are forced to be aligned by pixel-wise MSE loss. For images and prompts from the forget set, we pass noisy image and prompt to be forgotten to the U-net we are fine-tuning, and we pass a prompt from the overriding concept to the frozen U-net and force alignment with MSE loss on the score predictions. This way, when conditioned on unsafe prompt, the model learns to align itself to what the original model does when conditioned with safe concept.

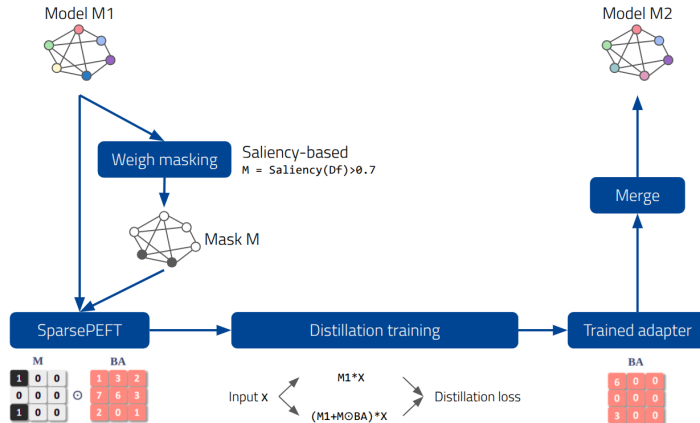
Let (x_r, p_r) be image-prompt pair from the retain set, (x_f, p_f) be image-prompt pair from the forget set, (p_o) be prompt from the overwrite set and $f(x, t, \epsilon)$ be the forward diffusion on x to time-step t with gaussian noise ϵ . Then ϕ is the original frozen model, θ is the model being finetuned and the self-distillation based objective becomes the following:

$$L = \mathbb{E}_{x_r, t, \epsilon} \left[\|\epsilon_\phi(f(x_r, t, \epsilon), p_r) - \epsilon_\theta(f(x_r, t, \epsilon), p_r)\|^2 \right] + \mathbb{E}_{x_f, t, \epsilon} \left[\|\epsilon_\phi(f(x_f, t, \epsilon), p_o) - \epsilon_\theta(f(x_f, t, \epsilon), p_f)\|^2 \right] \quad (1)$$

Where $\epsilon_\phi(\cdot)$ and $\epsilon_\theta(\cdot)$ represents the score prediction from the U-net of the corresponding models.

In order to leverage the sparse adapter obtained at step 1, we adapted the self-distillation for using LoRA. Furthermore, this method does not require maintaining a copy of the frozen model on the GPU, decreasing the VRAM usage, because it requires only enabling and disabling the LoRA module when needed: when we need the output of the original model, we disable the adapter and make the forward pass; when we want the output of the fine-tuned model, we enable the adapter.

Compared to the distillation scheme of Score Forgetting Distillation [23], our method calculates the loss directly on the image space, without using an auxiliary score network, since both teacher and student are computed for the same number of forward diffusion process steps. Compared to Concept Ablation [20], our method add a preservation term, similar to the idea proposed in Memory Replay GANs [52], thus improving the retention quality; Furthermore, our method does not rely on stopgrad to obtain the teacher’s prediction. After the training is completed, the trained adapter can be safely merged into the original model (Figure 1). This merge can be performed at runtime, and undone at any time, easing usage in production environments.



5 Method evaluation

To assess the proposed method, we performed quantitative and qualitative evaluations, as well as an interpretability analysis. The quantitative evaluation is based on the UnlearnCanvas benchmark [10], as this is a common base for evaluating different unlearning methods, especially for text-to-image generation. In the qualitative section, some examples of outputs are shown, displaying the capabilities

of the proposed unlearning method. The interpretability section explores the activations in the cross-attention layers of the model’s U-Net, showing what happens during the unlearning process.

5.1 Quantitative results

The UnlearnCanvas becnhmark contains a dataset formulated from pictures of different objects in various well-defined artistic styles, such as Van Gogh or Monet, as well as less concrete styles like Gorgeous Love or Vibrant Flow. In total, there are 50 styles and 20 classes or objects, and the main metrics for measuring the performance of unlearning are accuracy (obtained by image classifiers) and FID. The benchmark already provides the necessary checkpoints for testing the methods, being them a Stable Diffusion (SD) v1.5 trained on their dataset, and ViT classifiers for classes and styles. This way, all methods start the unlearning from the same base model, the SD 1.5 which was trained to generate all classes and styles.

The authors propose a set of metrics divided in different spheres of unlearning quality, including metrics related to unlearning performance, robustness to attacks, finer-scale unlearning, and sequential unlearning. Due to time and computing constraints, we concentrated our work in evaluating the unlearning performance.

The hyperparameters used to unlearn the models were empirically explored during experiments to develop the method. They are related to the LoRA adapter trained for unlearning, scheduler type, optimizer, learning rate, among others, as described in the Table 1. The results of testing other hyperparameter values are reported in Section 6. For this evaluation, no knowledge location was applied.

Table 1: Hyperparameters used to unlearn models in the UnlearnCanvas evaluation

Optimizer	AdamW	LoRA rank	4
AdamW beta1	0.9	LoRA alpha	4
AdamW beta 2	0.999	LoRA dropout	0.2
AdamW epsilon	1e-08	LoRA init weights	Gaussian
AdamW weighth decay	1e-2	Scheduler	constant
Learning Rate	1e-4	Maximum train steps	1550
Learning rate warmup steps	0	Random flip horizontally	yes
Batch size	4		

Our quantitative evaluation focused on analyzing our method alongside the results of other methods evaluated utilizing UnlearnCanvas. We focused on the basic unlearning metrics described in Table 2. In UnlearnCanvas the domains are considered as objects domain and styles domain. The accuracies are obtained by using the pretrained ViT-Large classifiers for objects and styles, which evaluate the images generated by the unlearned models. The image generation for the models is done by creating prompts for all possible combinations of objects and styles, and generating 5 images, corresponding to 5 different seeds for each possible combination.

Table 2: UnlearnCanvas metrics description

UA	Unlearning Accuracy: 100 - (accuracy in the forget concept)
IRA	In-domain Retain Accuracy: mean accuracy in the concepts to retain in the same domain as the forget
CRA	Cross-domain Retain Accuracy: mean accuracy in the concepts to retain in the domain not from the forget
FID	Fréchet Inception Distance: distance between the retain dataset distribution and the distribution of the images generated by the unlearned model (excluding the forget concept)

When forgetting one style, the UA is 100 minus the style classifier accuracy obtained from the images generated by the unlearned model in the forgotten style. The IRA is the style classifier mean accuracy for all the other styles, and the CRA is the mean accuracy from the objects classifier on the generated images. The FID computes the Fréchet Inception Distance between the original dataset,

excluding the unlearned concept (whether it is class or a style), and the generated images by the unlearned model.

Besides these metrics, the benchmark also brings runtime for unlearning and peak memory used during the training phase. Those metrics were evaluated separately, since they strongly depend on the GPU used to conduct the experiments. The UnlearnCanvas authors used NVIDIA RTX A6000 GPU’s, while our experiments were performed in both a NVIDIA V100 with 16 GB and a NVIDIA A100 with 40 GB, so the time and memory are not directly comparable with the ones reported by the UnlearnCanvas team.

Alongside the direct comparison among methods, it is important to consider that each method use a different set of assumptions. There are different categories of unlearning methods, based on where they apply unlearning and the type of data input they use for it. Some methods perform fine-tuning only in the text encoder, not updating the image generator. Certain methods are designated by their authors as “data-free” because they do not require input images, just prompts. However, they usually end up generating images with an auxiliary general text-to-image model, or they rely on the concepts already known by the model, meaning they use the model’s output (image or feature space) to the prompt, which authors usually refer to as model editing. While other methods require a captioned image dataset. Our method is categorized in the third group, as we use actual images for the unlearning. Our method and other State-of-the-Art methods for unlearning in image generation are categorized in Table 3; also, all of them were evaluated with the UnlearnCanvas benchmark.

Table 3: Different categories of methods according to unlearning scope and data requirements

Only modify text encoder	“Data-free” methods	Requires captioned dataset
SEOT [53]	ESD [54]	FMN [55]
	UCE [21]	SaLUn [7]
	CA [20]	EDiff [56]
	SPM [57]	SAeUron [58]
	SHS [59]	Ours
	Slug [8]	

Another important difference is that our method uses an overwriting concept, a strategy some of the other methods also use, sometimes with different nominations such as guiding concept in UCE. For the evaluation in UnlearnCanvas we defined the forget dataset as all images and captions containing the forget concept, and the retain set as all the other remaining images and captions. The overwriting concept is only a textual definition of another concept, in the same domain, randomly selected from the retain set. For instance, to forget Van Gogh style, the overwriting concept was randomly selected as Meta Physics.

The models were generated for all the concepts present in UnlearnCanvas, the results per class or style can be seen in Appendix B. Since all models used the same initial model and no parameter knowledge location mask was applied, the overhead memory caused by the LoRA adaptation was 3.1MB for all models; this considers that the adapter is not merged to the original model weights (case in which there would be no memory overhead). Using the average results, we can observe how our method behaves against other State-of-the-Art methods, shown in Table 4.

Table 4: Performance Metrics in UnlearnCanvas. For each metric, the best scoring method is highlighted in green, the second best in yellow, and the worst in red.

Method	Effectiveness									Efficiency		
	Style Unlearning			Object Unlearning			FID (↓)	Time (s) (↓)	Memory (GB) (↓)	Storage (GB) (↓)		
	UA (↑)	IRA (↑)	CRA (↑)	UA (↑)	IRA (↑)	CRA (↑)						
ESD [54]	98.58%	80.97%	93.96%	92.15%	55.78%	44.23%	65.55	6163	17.8	4.3		
FMN [55]	88.48%	56.77%	46.60%	45.64%	90.63%	73.46%	131.37	350	17.9	4.2		
UCE [21]	98.40%	60.22%	47.71%	94.31%	39.35%	34.67%	182.01	434	5.1	1.7		
CA [20]	60.82%	96.01%	92.70%	46.67%	90.11%	81.97%	54.21	734	10.1	4.2		
SaLUn [7]	86.26%	90.39%	95.08%	86.91%	96.35%	99.59%	61.05	667	30.8	4.0		
SEOT [53]	56.90%	94.68%	84.31%	23.25%	95.57%	82.71%	62.38	95	7.34	0.0		
SPM [57]	60.94%	92.39%	84.33%	71.25%	90.79%	81.65%	59.79	29700	6.9	4.0		
EDiff [56]	92.42%	73.91%	98.93%	86.67%	94.03%	48.48%	81.42	1567	27.8	4.0		
SHS [59]	95.84%	80.42%	43.27%	80.73%	81.15%	67.99%	119.34	1223	31.2	4.0		
SAeUron [58]	95.80%	99.10%	99.40%	78.82%	95.47%	95.58%	94.03	62.15	2.8	0.2		
Slug [8]	86.29%	84.59%	88.43%	75.43%	77.50%	81.18%	75.97	39	3.61	0.04		
Ours	99.96%	99.45%	98.16%	98.55%	97.88%	99.82%	54.36	2025.68*	20.57*	0.03		

For better visualization, Figure 2 plots the UA vs IRA and CRA, in which the ideal region is the right corner, where the highest UA and the highest IRA or CRA are located. It is possible to see that FADE stands out in this region. Interestingly, our method shows a very similar response to both style and object unlearning, which is not commonly seen between other methods.

Figure 3 shows Memory vs Time, but the comparison should take into account that the environments used for running the experiments are different; As such, we can observe that that there is a trade-off, but experiments in a standardized hardware should be performed to directly compare the efficiency of different methods.

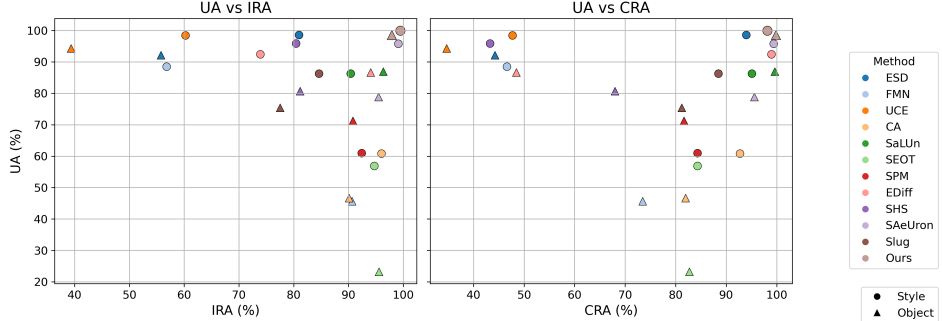


Figure 2: Unlearning accuracies by retaining accuracies for the methods shown in Table 4

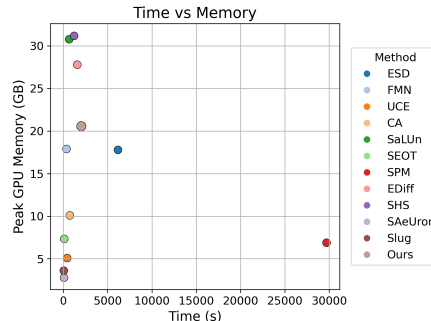


Figure 3: Peak memory during training by training runtime for the methods shown in Table 4

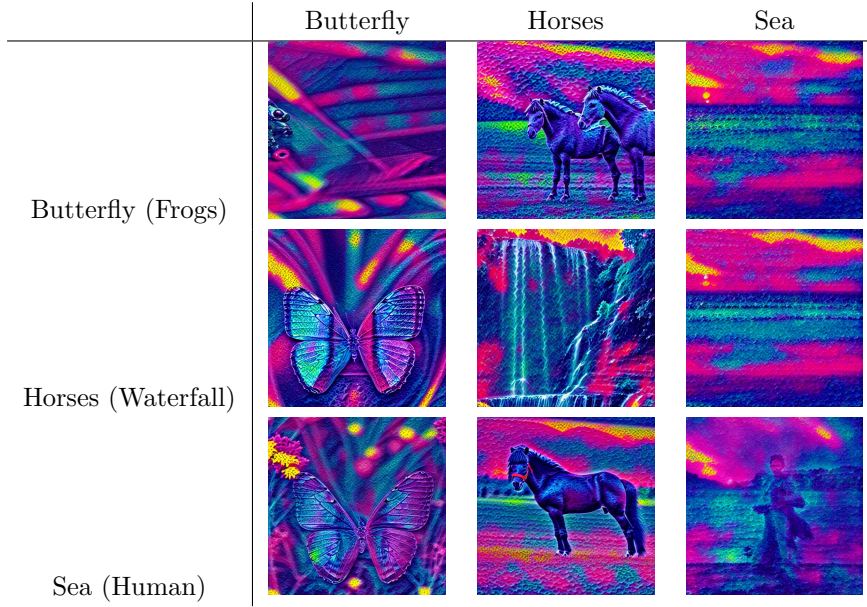


Figure 4: Examples of object forgetting under the Gorgeous Love style. The left column describes the unlearned model concept, in between brackets the overwriting concept used, and in the first row the object used in the prompt to sample the image.

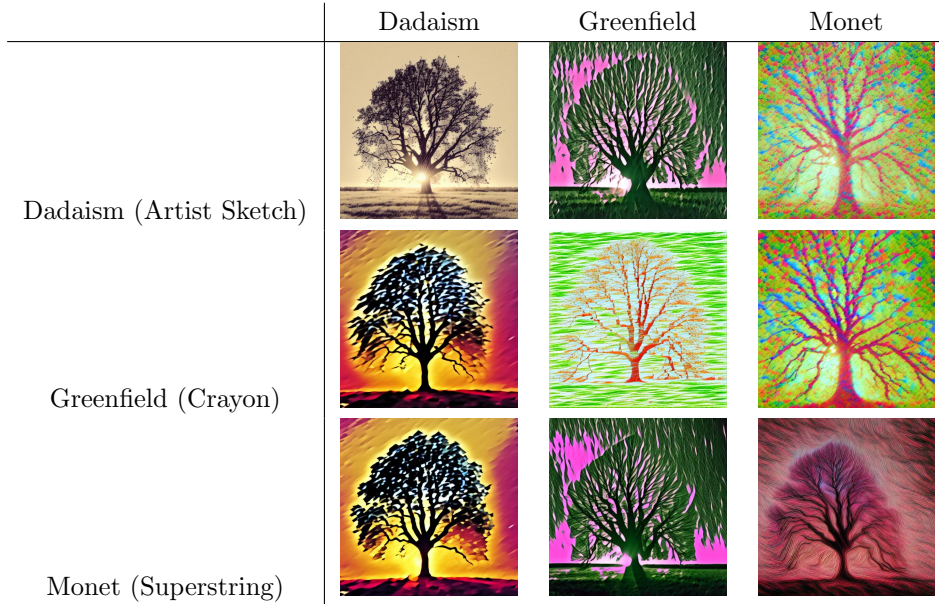


Figure 5: Examples of styles forgetting evaluated with the trees class. The left column describes the unlearned model concept, in between brackets the overwriting concept used, and in the first row the style used in the prompt to sample the image.

It is possible to notice that the styles in Figure 5 provided good forgetting characteristics. In the Figure 4 the results are slightly more complex: in the upper left corner the butterfly has disappeared, but the image does not present a clear object, which is acceptable for the purpose of forgetting. However, in many cases, the overwriting concept takes place, as in the image in the center, and in the butterfly case no frog is clearly identified. In the lower right corner another interesting case, the overwriting concept for sea was human, and clearly there is a human figure in the image, but in the background it is still possible to observe the sea.

Overall, FADE achieved better or similar performance to the highest scoring methods. Still, more

evaluations are needed to provide comparable efficiency metrics and a complete understanding its unlearning quality.

5.2 Qualitative results

We performed unlearning in several tasks to showcase the applicability of FADE in different contexts. Generated images were manually selected to be representative of the average unlearning quality obtained by FADE in the task. Across all tasks, and across several identities of each task and several concepts to be used for overwriting, FADE demonstrated impressive unlearning. A few selected examples are shown in Table 5, unlearning concepts from the datasets Labeled Faces in the Wild (LFW) [12], AtharvaTaras Dog Breeds Dataset [13], and SUN Attributes [14].

Task	Forget Concept	Overwrite Concept	Forget		Retain	
			Unlearned	Original	Unlearned	Original
People	George W. Bush	Kid				
	Dog breed					

Table 5: Qualitative results for forgetting and retention in 3 selected tasks.

5.3 Interpretability Analysis: Validating Concept Substitution via Cross-Attention

To rigorously verify the internal mechanism of our unlearning algorithm, we move beyond evaluating fully generated images and analyze the model’s intermediate representations. Specifically, we focus on the cross-attention layers within the diffusion model’s U-Net. In text-to-image diffusion models, cross-attention maps are responsible for aligning spatial image features with specific tokens from the input text prompt. By visualizing these maps, we can observe exactly which image regions the model associates with a specific concept, providing a transparent view into how the model interprets the token to be forgotten.

To create the attention maps of text tokens with the image tokens, we selected the 16x16 resolution level from the unet’s upsampling and downsampling blocks and analyzed the cross-attention values. Cross-attention between the text tokens and 16x16 resolution image tokens happens five times in a single forward pass through the Unet, two times in the downsampling path, and three times in the upsampling path, so we averaged the attention maps from these five instances. Also, since the cross-attention is multi-head attention, we average the attention maps across the heads. We also disregarded the cross-attention between the image tokens and the unconditional prompt used for classifier-free guidance. And finally, since the unet is used multiple times for one generation, we averaged the attention maps over the diffusion timesteps to get a final attention map for the generated image.

The efficacy of our “safe concept replacement” strategy is visibly demonstrated when comparing the attention maps before and after the unlearning process. We did the illustration for a model finetuned to forget how to generate gas pumps by overriding it with garbage trucks. As illustrated in the Figure 6, we visualize the activations corresponding to the target token (“gas pump”). We can see in the original model, the embedding of the “gas pump” token have high attention scores to the regions of the generated image that belongs to a gas pump, but after the fine-tuning the same tokens now have high scores for pixels belonging to a garbage truck. Also, we can see the difference in the attention maps is visible even from the first denoising step, where there is no semantic information coming from the image tokens, indicating that this change in the cross-attention map between the text and image tokens is the driving factor in the change of the model’s behavior. This visualization confirms that our algorithm has not merely suppressed the original concept but has successfully rewritten the semantic mapping in the model’s weights. Figure 7 further illustrates how the attention map of the “gas pump” token embeddings changes over the training steps.

6 Ablation studies

Due to the high computational costs of both unlearning and inference with diffusion models, many of the reported experiments utilize low number of unlearning sessions, as well as few evaluation metrics and generated images.

6.1 Impact of sparsity

The hyperparameter Q controls the number of most active parameters to undergo fine-tuning, with possible values ranging from 0 (no parameter is trained) to 1 (all parameters are trained). We experimented with 6 levels of sparsity, and the 2 different modes of defining sparsity (fine-grained per-weight masking and coarse-grained per-block masking).

We performed this experiment forgetting the object Gas Pump from Imagenette [11], replacing it by Truck, and evaluated using the CLIP-score between image and prompt and the unlearning runtime. Metrics are summarized in Figure 8, where we observe that: sparsity worsens the forgetting (we could intuitively interpret as making the unlearning more “narrow”); No clear impact on retaining was observed; The runtime increases as we finetune more parameters.

These results indicate that the benefits of sparsity are minor, and the main contribution of our method is the distillation training. These conclusions echo the ones from [31], that analyzed the impact (or lack of impact) of location strategies, concluding that failure of localized unlearning may stem from the absence of a uniquely responsible parameter region.

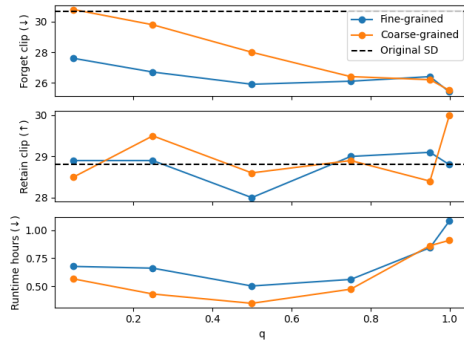
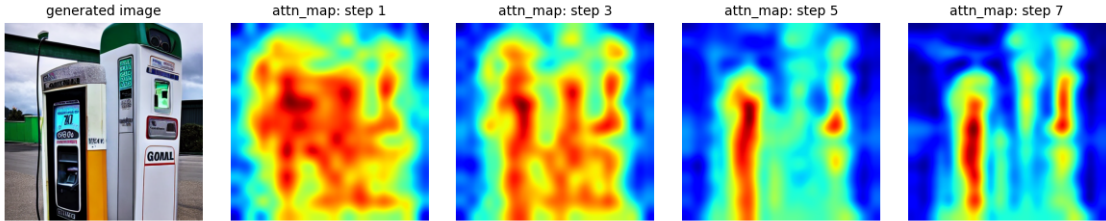


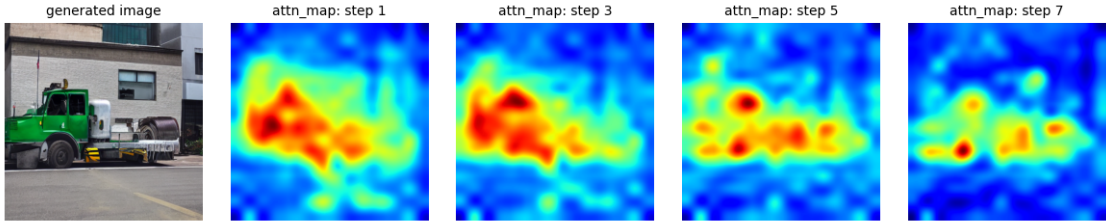
Figure 8: Sensitivity to the sparsity

6.2 Impact of overwrite concept

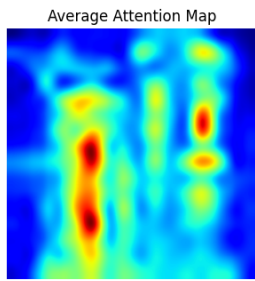
We hypothesize that the semantic proximity between the targeted forget concept and the selected safe surrogate is a somewhat important factor in the efficiency of the unlearning process. Specifically, choosing a surrogate concept that is semantically or structurally similar to the forget concept (e.g.,



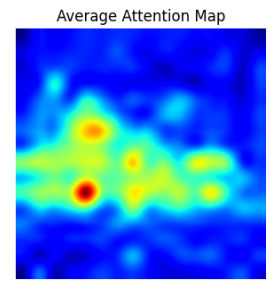
(a) Attention maps over diffusion timesteps (original model)



(b) Attention maps over diffusion timesteps (fine-tuned model)



(c) Mean attention map (original model)



(d) Mean attention map (fine-tuned model)

Figure 6: Comparison of attention maps between the token embedding of “gas pump” and the image tokens, between the original stable diffusion and a model finetuned to forget gas pump by overriding it with truck. The top two panels show attention maps across diffusion timesteps for each model, while the bottom panels show the mean attention maps aggregated over timesteps.

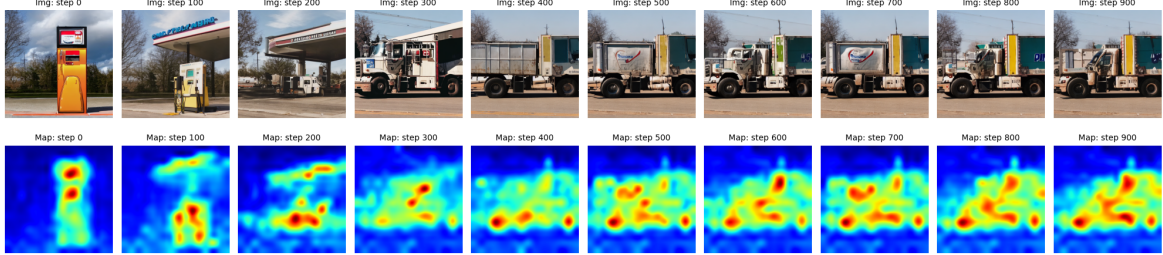


Figure 7: Attention map evolution across training steps: The figure illustrates the attention map of the token “gas pump” with the generated image tokens during the fine-tuning steps. We can observe the token starts attending more and more to pixels coming from the truck as we train for more steps

replacing “cat” with “dog” rather than “car”) allows the model to leverage overlapping feature representations in the latent space, thereby minimizing the magnitude of the required weight adjustments. Consequently, we expect that a higher degree of closeness will result in faster convergence during fine-tuning and superior retention of the model’s general capabilities, as the localized updates reduce the risk of distorting unrelated concepts (catastrophic forgetting).

To test the hypothesis, we experiment on the imagenette dataset by fine-tuning stable diffusion by replacing gas pump with each of the other nine classes and see how it performs based on the replacing concept used. To measure unlearning quality, we used FID-forget (FID between images generated by the model for the unlearned class and real images of the unlearned concept), FID-retain (FID between images generated for the other classes and real images from the other classes), CLIP-forget, and CLIP-retain. To measure similarity between two concepts, we used both text-based and image-based similarity measures. CLIP text-text similarity (T-T Sim), CLIP image-image similarity (T-I Sim), CLIP text-image similarity (I-I Sim), and FID between images of the two concepts (I-I Sim). Table 6 shows the results obtained. Based on the retain FID and CLIP, the pattern does not clearly confirm the hypothesis. Based on the four similarity metrics to compare the concepts, even though garbage truck was the closest in the three metrics, it doesn’t lead to better retain performance. In fact, the retain CLIP doesn’t seem to be affected at all by the selected replacement concept, while the FID shows some variation without a clear pattern.

Table 6: **Comparison of Replacement Concepts and Unlearning Performance.** The table relates the semantic and visual proximity of the replacing concept to the target (Gas Pump) with the final unlearning metrics. *Sim* denotes Cosine Similarity (higher is closer), *FID* denotes Fréchet Inception Distance (lower is closer distributions). *CLIP-F* and *FID-F* measure the forgetting of the target class, while *CLIP-R* and *FID-R* measure the retention of the other nine classes.

Replacing Concept	Concept Similarity (to “gas pump”)				Unlearning Performance			
	T-T Sim	T-I Sim	I-I Sim	I-I FID	CLIP-F ↓	FID-F ↑	CLIP-R ↑	FID-R ↓
Cassette Player	0.758	0.249	0.764	200.47	0.209	207.20	0.307	84.65
Chain Saw	0.771	0.272	0.812	346.58	0.240	221.39	0.307	86.51
Church	0.772	0.218	0.697	211.27	0.161	257.74	0.307	86.37
English Springer	0.737	0.222	0.628	227.02	0.202	224.97	0.307	85.55
French Horn	0.731	0.217	0.662	218.29	0.191	248.67	0.307	85.13
Garbage Truck	0.804	0.263	0.819	191.98	0.218	191.28	0.307	85.83
Golf Ball	0.758	0.219	0.688	220.27	0.197	237.39	0.307	86.33
Parachute	0.709	0.219	0.694	211.51	0.189	217.13	0.307	85.61
Tench	0.742	0.206	0.587	228.68	0.193	231.31	0.307	87.29

Furthermore, we analyzed how the choice of the replacing class affects the retaining ability of the model for each of the other classes individually, to identify for a selected replacing class, which other classes improves the most and degraded the worst. Table 7 shows the results. Every row represents a model where “gas pump” is replaced by the given replacing concept, and the columns shows the FID of the images generated for all nine retain classes.

Table 7: **Detailed Retention FID Scores per Replacing Concept.** The table shows the Fréchet Inception Distance (FID) for each of the nine retained classes. Green indicates the class with the most improvement (or least degradation) relative to the baseline. Red indicates the class with the most degradation relative to the baseline.

Replacing Concept	Cassette	Chain Saw	Church	Springer	Horn	Truck	Golf	Parachute	Tench
Cassette Player	78.24	229.05	83.88	64.87	56.02	60.74	37.31	48.84	102.89
Chain Saw	78.82	232.94	83.18	64.63	55.09	63.10	37.35	53.40	110.09
Church	81.10	226.18	81.63	68.40	55.47	62.28	38.14	52.88	111.28
English Springer	79.89	228.39	87.04	64.71	55.45	61.61	37.38	50.55	104.87
French Horn	82.00	225.10	81.80	64.30	55.61	63.68	37.69	49.67	106.35
Garbage Truck	79.04	234.91	82.38	63.82	55.23	63.05	37.49	51.26	105.27
Golf Ball	79.39	232.85	83.68	66.06	55.57	62.72	37.21	53.60	105.93
Parachute	81.23	226.59	84.95	65.51	55.35	62.78	37.33	50.76	105.96
Tench	80.07	238.64	84.58	65.25	55.51	63.40	36.82	49.81	111.50
Original SD (Baseline)	79.75	230.60	84.55	65.04	55.34	63.43	37.26	53.33	107.25

6.3 Unlearning rate and replacing concept

We analyzed how fast the unlearning and replacing happen during various unlearning sessions to observe if there are trends. Figure 9 shows how the CLIP-score between the gas pump generated images and the text “an image of gas pump” changes over time as we do the training saving the model every 100 steps. The plots also shows how the CLIP-score between the replacing concept and the images generated for gas pump gets higher over time. We can see that the CLIP-score decreases the fastest when gas pump was replaced by garbage truck, which was according to the similarity analysis done in the previous section the closest class to gas pump, implying that unlearning with a closer concept leads to faster unlearning.

6.4 Impact of other hyperparameters

Beyond the aforementioned elements of the proposed method, several other hyperparameters influence the quality of the results. In this section, we analyze the impact of the hyperparameters `learning_rate`, `lora_alpha`, `lora_dropout`, `lora_r`, and `max_grad_norm`. For each hyperparameter, 4-5 values were tried, holding all other hyperparameters constant, forgetting different identities (one at the time) from the LFW dataset [12]. Evaluation was performed measuring the difference in CLIP-score between the original model and the unlearned model for the same prompt and seed, for a small set of 4 prompts related to the forget concept (the identity to be unlearn) and 4 prompts related to retain concepts (other identities).

For the hyperparameter `max_grad_norm` (holding fixed `learning_rate=4e-4`, `lora_alpha=4`, `lora_dropout=0.1`, and `lora_r=4`, the results are reported in Figure 10.

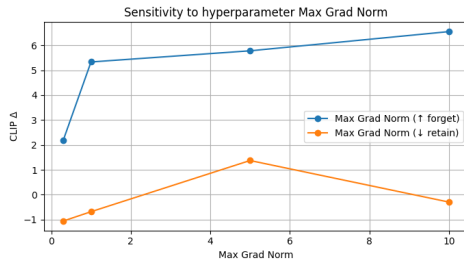


Figure 10: Sensitivity to the hyperparameter `max_grad_norm`

For the hyperparameter `lora_r` (holding fixed `learning_rate=4e-4`, `max_grad_norm=5.0`, `lora_alpha=4`, and `lora_dropout=0.1`), the results are reported in Figure 11. A good balance between forgetting and retaining is obtained around the value 32, after which the unlearning process becomes more damaging. Furthermore, a higher rank also implies a higher computational cost during training.

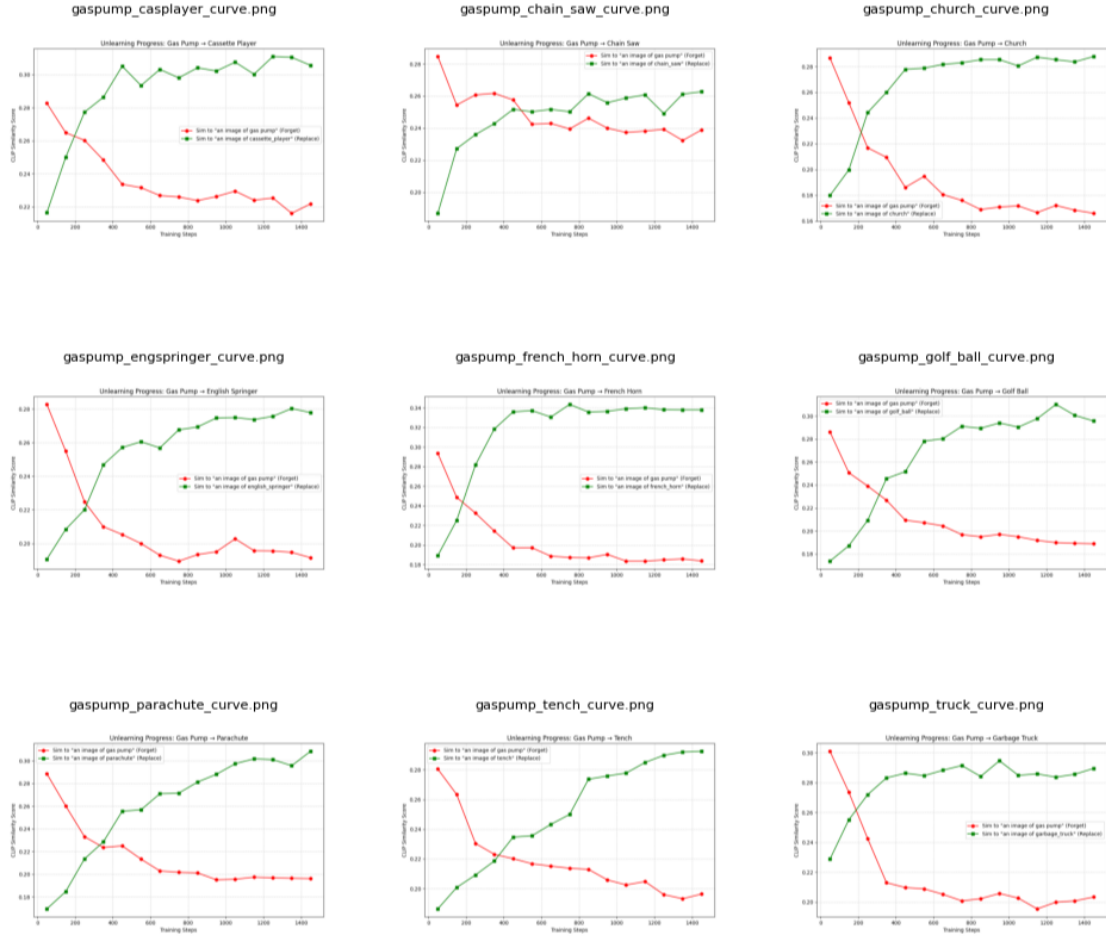


Figure 9: **Dynamics of Concept Replacement.** The plots illustrate the evolution of CLIP-score scores across training steps (50–1450). The red line shows the decreasing similarity to the target concept (“gas pump”), while the green line tracks the increasing similarity to the replacing concept. The steepness of these curves and the point of intersection indicate the relative speed at which each replacing concept overwrites the target.

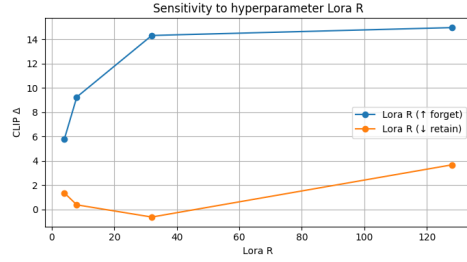


Figure 11: Sensitivity to the hyperparameter `lora_r`

For the hyperparameter `lora_dropout` (holding fixed `learning_rate=4e-4`, `max_grad_norm=5.0`, `lora_r=8`, and `lora_alpha=4`), the results are reported in Figure 12. With dropout higher than 0.2, the results worsen for both forget and retain scores.

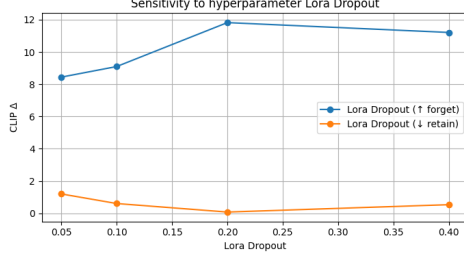


Figure 12: Sensitivity to the hyperparameter `lora_dropout`

For the hyperparameter `lora_alpha` (holding fixed `learning_rate`= $4\text{e-}4$, `max_grad_norm`=5.0, `lora_r`=8, and `lora_dropout`=0.2), the results are reported in Figure 13. Even though better metrics are observed for lower values of alpha (specially below 4), a careful examination of the generates images indicate worse naturalness and coherence, which is not always captured by the CLIP-score.

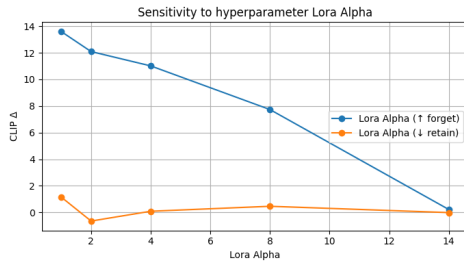


Figure 13: Sensitivity to the hyperparameter `lora_alpha`

For the hyperparameter `learning_rate` (holding fixed `max_grad_norm`=5.0, `lora_r`=8, `lora_dropout`=0.2, and `lora_alpha`=4), the results are reported in Figure 14. Values above $6\text{e-}4$ harm the unlearning process, specially in the retain set. Additionally, during the experiments we observed a relationship between the number of epochs and the learning rate, with similar results being obtained when the product between both hyperparameters is constant.

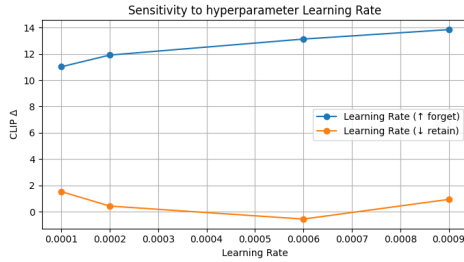


Figure 14: Sensitivity to the hyperparameter `learning_rate`

7 Conclusion

This paper presents FADE, a method for unlearning concepts in text-to-image stable diffusion models. Leveraging on LoRA adaptation, the model provides lightweight modules that enable the removal of the forget concept. The evaluations in UnlearnCanvas benchmark showed that our method improves upon the current State-of-the-Art methods.

It is important to point out that our evaluations are restricted to a few datasets such as Imagenette and UnlearnCanvas. Due to our method’s characteristic of overwriting a concept by another, the results might be sensitive to the choice of overwrite concept, a hypothesis which was not yet validated. Furthermore, the quantitative evaluations on UnlearnCanvas were restricted to simple unlearning per-

formance, and further testing are needed in order to assess the method’s robustness to sequential unlearning, knowledge revival, and adversarial attacks.

For a more equitable comparison, it would be important to run the experiments in the same GPU settings as the UnlearnCanvas evaluation, thus enabling the comparison of the efficiency metrics of our method. Besides that, exploration on other benchmarks, different models, and additional tasks such as style editing or image classification could promote broader adoption of the method. Explorations of the impact of overwriting choice as well as an automatic selection of concept would further enhance the capabilities of FADE. Lastly, FADE could theoretically be applied to architectures other than Stable Diffusion, but rigorous evaluation in that regard still needs to be performed.

References

- [1] T. Shaik, X. Tao, H. Xie, L. Li, X. Zhu, and Q. Li, “Exploring the landscape of machine unlearning: A comprehensive survey and taxonomy,” *IEEE Transactions on Neural Networks and Learning Systems*, pp. 1–21, 2024.
- [2] “Regulation (EU) 2016/679 of the European Parliament and of the Council of 27 April 2016 on the protection of natural persons with regard to the processing of personal data and on the free movement of such data, and repealing Directive 95/46/EC (General Data Protection Regulation).” <https://eur-lex.europa.eu/eli/reg/2016/679/oj>, 2016. OJ L 119, 4.5.2016, p. 1–88.
- [3] J. Zhang, S. Chen, J. Liu, and J. He, “Composing parameter-efficient modules with arithmetic operations,” 2023.
- [4] C. L. Choi, A. Duplessis, and S. Belongie, “Unlearning-based neural interpretations,” 2025.
- [5] H. Xu, T. Zhu, L. Zhang, W. Zhou, and P. S. Yu, “Machine unlearning: A survey,” *ACM Comput. Surv.*, vol. 56, Aug. 2023.
- [6] J. Ho, A. Jain, and P. Abbeel, “Denoising diffusion probabilistic models,” in *Advances in Neural Information Processing Systems* (H. Larochelle, M. Ranzato, R. Hadsell, M. Balcan, and H. Lin, eds.), vol. 33, pp. 6840–6851, Curran Associates, Inc., 2020.
- [7] C. Fan, J. Liu, Y. Zhang, D. Wei, E. Wong, and S. Liu, “Salun: Empowering machine unlearning via gradient-based weight saliency in both image classification and generation,” *arXiv preprint arXiv:2310.12508*, 2023.
- [8] Z. Cai, Y. Tan, and M. S. Asif, “Targeted unlearning with single layer unlearning gradient,” in *Forty-second International Conference on Machine Learning*, 2025.
- [9] L. Wang, X. Zeng, J. Guo, K.-F. Wong, and G. Gottlob, “Selective forgetting: Advancing machine unlearning techniques and evaluation in language models,” 2024.
- [10] Y. Zhang, C. Fan, Y. Zhang, Y. Yao, J. Jia, J. Liu, G. Zhang, G. Liu, R. Kompella, X. Liu, and S. Liu, “Unlearnncanvas: Stylized image dataset for enhanced machine unlearning evaluation in diffusion models,” in *Advances in Neural Information Processing Systems* (A. Globerson, L. Mackey, D. Belgrave, A. Fan, U. Paquet, J. Tomczak, and C. Zhang, eds.), vol. 37, pp. 96387–96423, Curran Associates, Inc., 2024.
- [11] J. Howard, “Imagenette.” <https://github.com/fastai/imagenette>, 2019. Accessed: 2025-05-21.
- [12] G. B. Huang, M. Mattar, T. Berg, and E. Learned-Miller, “Labeled Faces in the Wild: A Database for Studying Face Recognition in Unconstrained Environments,” in *Workshop on Faces in ‘Real-Life’ Images: Detection, Alignment, and Recognition*, (Marseille, France), Erik Learned-Miller and Andras Ferencz and Frédéric Jurie, Oct. 2008.
- [13] AtharvaTaras, “Dog-Breeds-Dataset: A dataset of images for dog breeds recognized by the fci.” <https://github.com/AtharvaTaras/Dog-Breeds-Dataset>, 2025. Accessed: 2025-12-11; licensed under CC-BY-4.0.
- [14] G. Patterson and J. Hays, “Sun attribute database: Discovering, annotating, and recognizing scene attributes,” in *2012 IEEE Conference on Computer Vision and Pattern Recognition*, pp. 2751–2758, June 2012.
- [15] R. Rombach, A. Blattmann, D. Lorenz, P. Esser, and B. Ommer, “High-resolution image synthesis with latent diffusion models,” *2022 IEEE/CVF Conference on Computer Vision and Pattern Recognition (CVPR)*, pp. 10674–10685, 2021.
- [16] L. Xu, H. Xie, S.-Z. J. Qin, X. Tao, and F. L. Wang, “Parameter-efficient fine-tuning methods for pretrained language models: A critical review and assessment,” 2023.

- [17] E. J. Hu, Y. Shen, P. Wallis, Z. Allen-Zhu, Y. Li, S. Wang, L. Wang, and W. Chen, “Lora: Low-rank adaptation of large language models,” 2021.
- [18] J. P. Munoz, J. Yuan, and N. Jain, “SQFT: Low-cost model adaptation in low-precision sparse foundation models,” in *Findings of the Association for Computational Linguistics: EMNLP 2024* (Y. Al-Onaizan, M. Bansal, and Y.-N. Chen, eds.), (Miami, Florida, USA), pp. 12817–12832, Association for Computational Linguistics, Nov. 2024.
- [19] Y. Cao and J. Yang, “Towards making systems forget with machine unlearning,” in *2015 IEEE Symposium on Security and Privacy*, pp. 463–480, May 2015.
- [20] N. Kumari, B. Zhang, S.-Y. Wang, E. Shechtman, R. Zhang, and J.-Y. Zhu, “Ablating concepts in text-to-image diffusion models,” in *International Conference on Computer Vision (ICCV)*, 2023.
- [21] R. Gandikota, H. Orgad, Y. Belinkov, J. Materzyńska, and D. Bau, “Unified concept editing in diffusion models,” in *Proceedings of the IEEE/CVF Winter Conference on Applications of Computer Vision*, 2024. arXiv:2308.14761.
- [22] J. Huo, Y. Yan, X. Zheng, Y. Lyu, X. Zou, Z. Wei, and X. Hu, “MMUnlearner: Reformulating multimodal machine unlearning in the era of multimodal large language models,” in *Findings of the Association for Computational Linguistics: ACL 2025* (W. Che, J. Nabende, E. Shutova, and M. T. Pilehvar, eds.), (Vienna, Austria), pp. 7190–7206, Association for Computational Linguistics, July 2025.
- [23] T. Chen, S. Zhang, and M. Zhou, “Score forgetting distillation: A swift, data-free method for machine unlearning in diffusion models,” 2025.
- [24] L. C. Comas, “Machine unlearning: Fisher information matrix and selective forgetting in deep networks,” June 2024. Bachelor’s thesis, Facultat d’Informàtica de Barcelona (FIB).
- [25] J. Martens and R. Grosse, “Optimizing neural networks with kronecker-factored approximate curvature,” 2015.
- [26] S. P. Singh and D. Alistarh, “Woodfisher: Efficient second-order approximation for neural network compression,” 2020.
- [27] X. Liu, M. Masana, L. Herranz, J. Van de Weijer, A. M. López, and A. D. Bagdanov, “Rotate your networks: Better weight consolidation and less catastrophic forgetting,” in *2018 24th International Conference on Pattern Recognition (ICPR)*, pp. 2262–2268, Aug 2018.
- [28] A. Golatkar, A. Achille, and S. Soatto, “Eternal sunshine of the spotless net: Selective forgetting in deep networks,” in *2020 IEEE/CVF Conference on Computer Vision and Pattern Recognition (CVPR)*, pp. 9301–9309, June 2020.
- [29] Z. Izzo, M. A. Smart, K. Chaudhuri, and J. Y. Zou, “Approximate data deletion from machine learning models: Algorithms and evaluations,” *CoRR*, vol. abs/2002.10077, 2020.
- [30] J. Frankle and M. Carbin, “The lottery ticket hypothesis: Finding sparse, trainable neural networks,” in *International Conference on Learning Representations (ICLR)*, OpenReview.net, 2019. Published conference version; see also arXiv:1803.03635.
- [31] H. Lee, U. Hwang, H. Lim, and T. Kim, “Does localization inform unlearning? a rigorous examination of local parameter attribution for knowledge unlearning in language models,” 2025.
- [32] N. Yang, M. Kim, S. Yoon, J. Shin, and K. Jung, “Faithun: Toward faithful forgetting in language models by investigating the interconnectedness of knowledge,” 2025.
- [33] Z. Liu, G. Dou, X. Yuan, C. Zhang, Z. Tan, and M. Jiang, “Modality-aware neuron pruning for unlearning in multimodal large language models,” 2025.
- [34] J. Jia, J. Liu, P. Ram, Y. Yao, G. Liu, Y. Liu, P. Sharma, and S. Liu, “Model sparsity can simplify machine unlearning,” in *Proceedings of the 37th International Conference on Neural Information Processing Systems*, NIPS ’23, (Red Hook, NY, USA), Curran Associates Inc., 2024.

[35] G. E. Hinton, O. Vinyals, and J. Dean, “Distilling the knowledge in a neural network,” *ArXiv*, vol. abs/1503.02531, 2015.

[36] B. W. Lee, A. Foote, A. Infanger, L. Shor, H. Kamath, J. Goldman-Wetzler, B. Woodworth, A. Cloud, and A. M. Turner, “Distillation robustifies unlearning,” 2025.

[37] Y. Quan, Z. Li, and G. Montana, “Efficient verified machine unlearning for distillation,” 2025.

[38] Y. Zhou, D. Zheng, Q. Mo, R. Lu, K.-Y. Lin, and W.-S. Zheng, “Decoupled distillation to erase: A general unlearning method for any class-centric tasks,” in *Proceedings of the IEEE/CVF Conference on Computer Vision and Pattern Recognition (CVPR)*, pp. 20350–20359, June 2025.

[39] N. George, K. N. Dasaraju, R. R. Chittepu, and K. R. Mopuri, “The illusion of unlearning: The unstable nature of machine unlearning in text-to-image diffusion models,” in *Proceedings of the IEEE/CVF Conference on Computer Vision and Pattern Recognition (CVPR)*, pp. 13393–13402, June 2025.

[40] M. Heusel, H. Ramsauer, T. Unterthiner, B. Nessler, and S. Hochreiter, “Gans trained by a two time-scale update rule converge to a local nash equilibrium,” 2018.

[41] A. Radford, J. W. Kim, C. Hallacy, A. Ramesh, G. Goh, S. Agarwal, G. Sastry, A. Askell, P. Mishkin, J. Clark, G. Krueger, and I. Sutskever, “Learning transferable visual models from natural language supervision,” in *Proceedings of the 38th International Conference on Machine Learning* (M. Meila and T. Zhang, eds.), vol. 139 of *Proceedings of Machine Learning Research*, pp. 8748–8763, PMLR, 18–24 Jul 2021.

[42] C.-P. Huang, K.-P. Chang, C.-T. Tsai, Y.-H. Lai, F.-E. Yang, and Y.-C. F. Wang, “Receler: Reliable concept erasing of text-to-image diffusion models via lightweight erasers,” in *Computer Vision – ECCV 2024* (A. Leonardis, E. Ricci, S. Roth, O. Russakovsky, T. Sattler, and G. Varol, eds.), (Cham), pp. 360–376, Springer Nature Switzerland, 2025.

[43] I. Prempidis, M. Lymperaiou, G. Filandrianos, O. M. Mastromichalakis, A. Voulovodimos, and G. Stamou, “Ails-ntua at semeval-2025 task 4: Parameter-efficient unlearning for large language models using data chunking,” 2025.

[44] X. Wang, Z. Li, B. Wang, Y. Hu, and D. Zou, “Model unlearning via sparse autoencoder subspace guided projections,” 2025.

[45] S. Lu, Z. Wang, L. Li, Y. Liu, and A. W.-K. Kong, “Mace: Mass concept erasure in diffusion models,” in *Proceedings of the IEEE/CVF Conference on Computer Vision and Pattern Recognition (CVPR)*, pp. 6430–6440, June 2024.

[46] R. Liu, W. Feng, T. Zhang, W. Zhou, X. Cheng, and S.-K. Ng, “Rethinking machine unlearning in image generation models,” 2025.

[47] S. Moon, M. Lee, S. Park, and D. Kim, “Holistic unlearning benchmark: A multi-faceted evaluation for text-to-image diffusion model unlearning,” *arXiv preprint arXiv:2410.05664*, 2024.

[48] D. Chen, Z. Li, C. Chen, Y. Xie, X. Li, J. Ye, Y. Chen, and Y. Li, “Comprehensive evaluation and analysis for nsfw concept erasure in text-to-image diffusion models,” 2025.

[49] V. M. Suriyakumar, R. Alur, A. Sekhari, M. Raghavan, and A. C. Wilson, “Unstable unlearning: The hidden risk of concept resurgence in diffusion models,” 2025.

[50] J. Lee, S. Yu, Y. Jang, S. S. Woo, and J. Jo, “Unlearning comparator: A visual analytics system for comparative evaluation of machine unlearning methods,” 2025.

[51] L. S. B. Pereira, “sparse-peft.” <https://github.com/LeonardoSanBenitez/sparse-peft>, 2025. Accessed: 2025-11-29.

[52] C. Wu, L. Herranz, X. Liu, y. wang, J. van de Weijer, and B. Raducanu, “Memory replay gans: Learning to generate new categories without forgetting,” in *Advances in Neural Information Processing Systems* (S. Bengio, H. Wallach, H. Larochelle, K. Grauman, N. Cesa-Bianchi, and R. Garnett, eds.), vol. 31, Curran Associates, Inc., 2018.

- [53] S. Li, J. van de Weijer, taihang Hu, F. Khan, Q. Hou, Y. Wang, and jian Yang, “Get what you want, not what you don’t: Image content suppression for text-to-image diffusion models,” in *The Twelfth International Conference on Learning Representations*, 2024.
- [54] R. Gandikota, J. Materzynska, J. Fiotto-Kaufman, and D. Bau, “Erasing concepts from diffusion models,” *2023 IEEE/CVF International Conference on Computer Vision (ICCV)*, pp. 2426–2436, 2023.
- [55] G. Zhang, K. Wang, X. Xu, Z. Wang, and H. Shi, “Forget-me-not: Learning to forget in text-to-image diffusion models,” in *Proceedings of the IEEE/CVF Conference on Computer Vision and Pattern Recognition (CVPR) Workshops*, pp. 1755–1764, June 2024.
- [56] J. Wu, T. Le, M. Hayat, and M. Harandi, “Erasediff: Erasing data influence in diffusion models,” 2024.
- [57] M. Lyu, Y. Yang, H. Hong, H. Chen, X. Jin, Y. He, H. Xue, J. Han, and G. Ding, “One-dimensional adapter to rule them all: Concepts, diffusion models and erasing applications,” in *IEEE/CVF Conference on Computer Vision and Pattern Recognition (CVPR)*, pp. 7559–7568, 06 2024.
- [58] B. Cywiński and K. Deja, “Saeuron: Interpretable concept unlearning in diffusion models with sparse autoencoders,” in *Forty-second International Conference on Machine Learning*, 2025.
- [59] J. Wu and M. Harandi, “Scissorhands: Scrub data influence via connection sensitivity in networks,” in *Computer Vision – ECCV 2024* (A. Leonardis, E. Ricci, S. Roth, O. Russakovsky, T. Sattler, and G. Varol, eds.), (Cham), pp. 367–384, Springer Nature Switzerland, 2025.
- [60] T. Oikarinen and T.-W. Weng, “Clip-dissect: Automatic description of neuron representations in deep vision networks,” *International Conference on Learning Representations*, 2023.
- [61] G. Goh, N. C. †, C. V. †, S. Carter, M. Petrov, L. Schubert, A. Radford, and C. Olah, “Multimodal neurons in artificial neural networks,” *Distill*, 2021. <https://distill.pub/2021/multimodal-neurons>.

A Ethical considerations

The development of machine unlearning methods is closely connected to privacy regulation frameworks such as the GDPR [2], which explicitly grants data subjects the right to erasure and imposes obligations on data controllers to ensure that personal data can be removed from deployed systems. Even though our method can, in principle, be used to comply with such regulations, no guarantees can be provided about the proper erasure of sensitive information. The authors bear no liability for the misuse of our method or derived works.

The capability to erase information also carries potential misuse risks. Unlearning can, in principle, be applied to hide wrongdoing, suppress forensic evidence, or tamper with model behavior in ways that undermine accountability. This risk is amplified when the unlearning method allows reversible manipulation through lightweight modules such as PEMs: approaches that enable inversion or re-application of a forgotten concept raise concerns about providing a false sense of deletion, where the information is not truly eliminated but merely modularized [3]. Therefore, we recommend any deployment of unlearned models to document their guarantees and limitations, avoid presenting approximate removal as absolute deletion, and consider governance mechanisms that deter malicious use while supporting legitimate privacy rights.

B Results for FADE in UnlearnCanvas

The tables 8 and 9 show the accuracy results and FID values computed for each unlearned model according to the forget concept.

Table 8: Style unlearning results

Theme	UA	IRA	CRA	FID	Theme	UA	IRA	CRA	FID
Abstractionism	100.00%	98.86%	98.84%	55.57	Magic Cube	100.00%	99.78%	98.59%	54.46
Artist Sketch	100.00%	99.70%	98.08%	55.05	Meta Physics	100.00%	99.72%	98.35%	54.34
Blossom Season	100.00%	99.56%	98.08%	53.67	Meteor Shower	100.00%	99.74%	98.25%	53.66
Bricks	100.00%	99.32%	98.29%	54.44	Monet	100.00%	99.34%	98.22%	53.59
Byzantine	99.00%	97.84%	96.80%	52.14	Mosaic	100.00%	99.90%	97.69%	54.30
Cartoon	100.00%	99.72%	97.84%	54.74	Neon Lines	100.00%	99.48%	98.59%	55.13
Cold Warm	100.00%	97.74%	97.73%	54.41	On Fire	100.00%	99.82%	98.49%	55.22
Color Fantasy	100.00%	99.68%	98.45%	54.18	Pastel	100.00%	99.60%	97.96%	53.56
Comic Etch	100.00%	99.68%	98.22%	52.91	Pencil Drawing	100.00%	99.50%	98.16%	54.83
Crayon	100.00%	96.98%	97.06%	54.37	Picasso	100.00%	99.66%	98.08%	53.45
Cubism	100.00%	99.72%	98.39%	52.23	Pop Art	100.00%	99.64%	98.18%	53.75
Dadaism	100.00%	99.44%	97.69%	53.21	Red Blue Ink	100.00%	99.56%	97.96%	54.50
Dapple	100.00%	99.62%	98.49%	55.03	Rust	100.00%	99.72%	98.00%	53.38
Defoliation	100.00%	99.70%	98.65%	55.72	Sketch	100.00%	99.56%	98.31%	54.84
Early Autumn	100.00%	99.66%	98.24%	54.96	Sponge Dabbed	100.00%	99.80%	98.33%	53.72
Expressionism	100.00%	99.26%	98.37%	54.02	Structuralism	100.00%	99.54%	97.67%	56.62
Fauvism	100.00%	99.62%	98.45%	54.26	Superstring	100.00%	99.74%	98.22%	53.92
French	100.00%	99.78%	98.04%	54.70	Surrealism	100.00%	99.48%	98.20%	52.32
Glowing Sunset	100.00%	99.66%	98.53%	54.22	Ukiyoe	100.00%	99.64%	98.35%	55.19
Gorgeous Love	100.00%	98.16%	98.47%	54.39	Van Gogh	100.00%	99.54%	98.45%	54.34
Greenfield	100.00%	99.68%	97.84%	53.47	Vibrant Flow	100.00%	99.70%	97.90%	56.76
Impressionism	100.00%	99.30%	97.43%	52.82	Warm Love	100.00%	99.70%	98.53%	54.45
Ink Art	100.00%	99.64%	98.29%	52.89	Warm Smear	100.00%	99.32%	98.06%	53.55
Joy	100.00%	99.86%	98.63%	54.60	Watercolor	99.00%	99.80%	98.41%	54.10
Liquid Dreams	100.00%	99.54%	97.92%	53.83	Winter	100.00%	99.48%	98.04%	51.82
					Average	99.96%	99.45%	98.16%	54.15

Table 9: Object unlearning results

Class	UA	IRA	CRA	FID	Class	UA	IRA	CRA	FID
Architectures	100.00%	98.43%	99.88%	54.06	Horses	100.00%	98.04%	99.82%	54.58
Bears	100.00%	98.06%	99.84%	53.44	Human	98.04%	98.20%	99.90%	56.90
Birds	100.00%	97.98%	99.78%	53.56	Jellyfish	100.00%	97.92%	99.90%	54.09
Butterfly	83.53%	97.50%	99.63%	55.37	Rabbits	100.00%	97.56%	99.84%	53.96
Cats	100.00%	97.83%	99.78%	54.86	Sandwiches	100.00%	97.23%	99.84%	56.62
Dogs	100.00%	98.02%	99.86%	54.31	Sea	96.86%	97.13%	99.71%	53.62
Fishes	100.00%	97.19%	99.75%	54.62	Statues	100.00%	98.60%	99.80%	55.23
Flame	99.61%	97.65%	99.80%	53.73	Towers	100.00%	98.16%	99.94%	54.14
Flowers	100.00%	98.37%	99.88%	54.03	Trees	92.94%	98.29%	99.90%	55.35
Frogs	100.00%	97.52%	99.86%	53.94	Waterfalls	100.00%	97.96%	99.69%	55.05
					Average	98.55%	97.88%	99.82%	54.57

C Interplay between sparsity and overwriting

The mechanism of knowledge location (reviewed in Section 2.3.2) was never, to the best of our knowledge, used together with knowledge overwriting ideas (Section 2.3.3). Even though both mechanisms can be utilized separately, it is reasonable to assume they influence one another, specially regarding the level of sparsity and the semantic distance between the forget and overwrite concepts. In this section we present a tentative theoretical framework to analyze this relationship.

On a conceptual level, we can hypothetically define W_o as the subset of weights that are related to D_o and similar for W_f . Such subset of weights could be identified in practice using the method proposed by [60, 61]. We would expect W_o to have at least some intersection with W_f in order to achieve optimal unlearning, as illustrated in Figure 15 Part 1. Similarly, if there is no overlap, the concept D_o would have to be learned from scratch within W_f during the unlearning process, which we hypothesize would be harder and/or slower to perform. We intend to systematically analyze this conjuncture in future works.

During fine-tuning, our method aligns the representations of D_f with safe concepts in D_o (Figure 15 Part 2, conceptually depicted as arrows into $W_o \cap W_f$). We hypothesize that this is performed in such a way that the parameters $W_o \cap W_f$ will, after unlearning, encode only information about D_o that resemble D_f (but is not recognizable as D_f anymore); The parameters $W_o \setminus W_f$ will remain unchanged, preserving the generation quality in the retain task, while $W_f \setminus W_o$ will likely be reused to encode other forms of useful knowledge for the retain task; The rest of the network, by design, remain unchanged. If this hypothesis is true, then the unlearning process is being done in an “optimal transport” manner, with the neurons in the unlearned model being utilized for generative tasks that are the semantically closest to the tasks they were used for before unlearning. Again, unlearning would likely be harder and/or slower to perform if the hypothesis is false.

On the light of this analysis, the very method used to define W_f could be adjusted to ensure unlearning optimality. One possibility would be selecting γ such that $W_f \cap W_o \neq \emptyset$, or by enlarging W_f with the closest parameters of W_o .

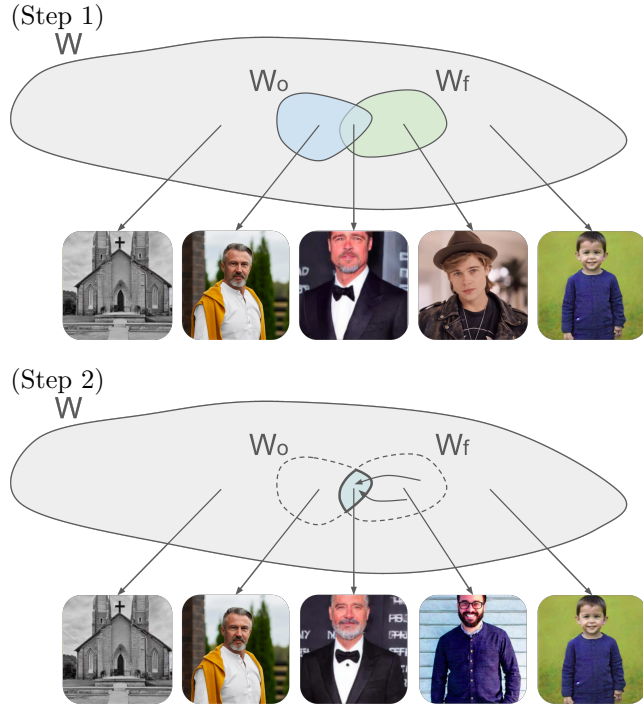


Figure 15: Example of replacing Brad Pitt by a common middle age man. Before unlearning (figure on top), W_o is subset of weights relevant for generating middle aged men and W_f is subset of weights relevant for generating Brad Pitt and there is some overlap between the two. After unlearning, weights in $W_o \setminus W_f$ are still relevant for generating middle aged men, weights in $W_o \cap W_f$ will be specialized for generating middle aged men that resembles Brad Pitt but not Brad Pitt (the alignment the representations is conceptually depicted as arrows into $W_o \cap W_f$), and the weights in $W_f \setminus W_o$ will be used for retaining other concepts. Images and proportions are for illustration purposes only.